45. We thank E. Borowicz, I. Leznicki, and A. Roth for technical assistance and R. Malenka, H. Krämer, F. Schmitz, A. Ho, S. Butz, A. Chubykin, and S. Chandra for advice and reagents. The sequence encoding mouse synCAM1 has been deposited in GenBank (accession number AF539424). E.T.K. is the Effie Marie Cain Endowed Scholar in Biomedical Research at the University of Texas Southwestern Medical Center. Supported by a grant from the NIH to T.C.S. (RO1-MH52804) and a postdoctoral fellowship from the Human Frontier Science Program (to T.B.).

Supporting Online Material
www.sciencemag.org/cgi/content/full/297/5586/1525/DC1
Materials and Methods
SOM Text
Figs. S1 to S12
29 March 2002; accepted 30 July 2002

The Mechanism of Diamond Nucleation from Energetic Species

Y. Lifshitz,[1,*†] Th. Köhler,[2] Th. Frauenheim,[2] I. Guzmann,[3‡] A. Hoffman,[3] R. Q. Zhang,[1] X. T. Zhou,[1] S. T. Lee[1]

A model for diamond nucleation by energetic species (for example, bias-enhanced nucleation) is proposed. It involves spontaneous bulk nucleation of a diamond embryo cluster in a dense, amorphous carbon hydrogenated matrix; stabilization of the cluster by favorable boundary conditions of nucleation sites and hydrogen termination; and ion bombardment–induced growth through a preferential displacement mechanism. The model is substantiated by density functional tight-binding molecular dynamics simulations and an experimental study of the structure of bias-enhanced and ion beam–nucleated films. The model is also applicable to the nucleation of other materials by energetic species, such as cubic boron nitride.

The exciting possible applications of diamond (*1–3*) motivated its high-pressure, high-temperature production half a century ago (*4*). Since then, chemical vapor deposition (CVD) methods have been developed to facilitate diamond growth at sub-atmospheric pressures, typically applying a hydrocarbon-hydrogen plasma (<1% hydrocarbon) over a substrate held at ~700° to 800°C. Diamond growth on diamond is relatively well understood and controlled. Diamond growth on non-diamond surfaces requires a nucleation step that is much less understood (*5*) and relies largely on trial and error.

The most controlled diamond nucleation method is biased enhanced nucleation (BEN) (*6, 7*), in which the substrate is negatively biased to ~100 to 200 V and exposed to the CVD plasma. The impingement of energetic plasma species induces the nucleation of diamond (*8–12*). Nucleation can be achieved in a similar way with direct ion beam bombardment (*13*).

Two nucleation sites associated with diamond formation in BEN have been identified: graphitic edges (*8, 11, 14*), for randomly oriented diamond, and steps, for heteroepitaxial (oriented) growth on Si (*12*). The actual nucleation process (the formation of a diamond cluster and its subsequent growth to form a stable crystallite) remains unresolved. Here we propose a model of the diamond nucleation process from energetic species (e.g., BEN). Each step in the model is substantiated by experimental data and molecular dynamics (MD) simulation results, as well as reported data and simulations for carbon systems not associated with BEN.

We propose that diamond nucleation via BEN is an internal (bulk) process that occurs in subsurface layers, ~1 to 2 nm below the surface, and advances as follows:

1) Step **a**. Formation of a dense amorphous hydrogenated carbon (a-C:H) phase (~1 to 2 nm thick) via a subplantation (*15–17*) process, wherein energetic carbon, hydrocarbon, and hydrogen species bombard the surface and are subsequently stopped and incorporated in subsurface layers. The density of this phase increases with subplantation until it reaches saturation.

2) Step **b**. Spontaneous precipitation of pure sp^3 carbon clusters containing tens of atoms in the a-C:H phase, induced by the "thermal spike" (*15–17*) of the impinging energetic species. Most clusters are amorphous, but a few (~1 in 10^4 to 10^6) are perfect diamond clusters. The formation probability of diamond clusters is increased by favorable boundary conditions of nucleation sites

3) Step **c**. Annealing of faults in defective clusters by incorporation of carbon "interstitials" in reactive sites and by hydrogen termination. Carbon interstitials and hydrogen atoms are provided through the subplantation process. Note that the amorphous matrix contains ~20 to 30% of hydrogen by atom (at%H).

4) Step **d**. Growth of diamond clusters to several nm (10^4 to 3×10^4 atoms) through transformation of amorphous carbon to diamond at the amorphous matrix-diamond interface. The transformation is induced by a "preferential displacement" mechanism (*15–17*) caused mainly by the impact of energetic hydrogen atoms. In this process, loosely bound amporphous carbon (a-C) atoms move to new diamond positions, leaving the more rigid diamond atoms unchanged. Under typical BEN conditions, the number of energetic hydrogen atoms is two orders of magnitude larger than that of energetic carbon ions, so each carbon atom in the amorphous phase should be bombarded and displaced many times.

Our model differs in two respects from previous attempts to understand the BEN process. First, we suggest that nucleation is a bulk not a surface process, which makes boundary conditions (*15–17*) important rather than surface energy effects. We also emphasize that diamond clusters growing on the substrate surface would be annihilated or graphitized by the bombarding energetic species. Second, we assume diamond nucleation to be a highly improbable event, which means the diamond may precipitate even under conditions in which the thermodynamic stability of diamond is lower than that of graphite.

Several major obstacles have previously hampered the elucidation of diamond nucleation mechanisms. First, small diamond clusters of ~30 atoms cannot be observed by experimental techniques, leaving simulation as the only means to observe them. Second, the very low probability of the formation of a perfect diamond cluster (which is still sufficient to facilitate the experimental nucleation densities) requires a large number (>10^4) of cell calculations for it to be observed, calculations that cannot be performed by currently available computers. We overcome these problems by suggesting that the formation of a perfect diamond cluster among many other faulty sp^3 clusters is statistically possible.

Evidence for each of the above steps is found both in new [supporting online material (SOM) Notes 1 to 3] and previously reported data. We first focus on the precursor material (step **a**) in which diamond later precipitates (step **b**) under optimal BEN conditions (*18*). High-resolution transmission electron microscopy (HRTEM) measurements (Fig. 1) prove the precipitation of diamond crystallites in this matrix and the formation of nucleation sites [silicon

[1]Center of Super Diamond and Advanced Films and Department of Physics and Materials Science, City University Hong Kong, Hong Kong SAR. [2]Universitäte/Gesamthochschule Paderborn, D-33095 Paderborn, Germany. [3]Department of Chemistry, Technion, Haifa 32000, Israel.

*To whom correspondence should be addressed. E-mail: apshay@cityu.edu.hk
†On leave from Soreq NRC, Yavne 81800, Israel.
‡Present address: Soreq NRC, Yavne 81800, Israel.

steps (*12*) or graphitic edges SOM Note 4]. Elastic recoil detection analysis (ERDA) measurements show that films with a large concentration of diamond nuclei contain substantial amounts of hydrogen. The films with the highest nucleation density ($\sim 10^{10}$ crystallites per cm^2) were deposited at 880°C, contained ~19 at%H, and had a density of 2.8g/cm^3 (SOM Note 5).

We now address step **b**, the spontaneous precipitation of sp^3 carbon clusters. We have calculated the structure of an a-C:H cell consisting of 128 carbon and 43 hydrogen atoms with a density of 3g/cm^3 and 25 at%H with density functional tight binding (DFTB) molecular dynamics (MD) simulations (SOM Note 3) (*19–22*). The calculations (Fig. 2A) show that the cell is predominantly tetrahedral, with an average C-C coordination number of 3.5 (compared with 4 for a fully tetrahedral structure). The number of sp^3-sp^3 C–C bonds (178) exceeds that of sp^3-sp^2 (34) and sp^2-sp^2 (7) bonds. The cell is nevertheless highly inhomogeneous. The marked hydrogen-free cluster in Fig. 2A containing 27 carbon atoms resembles a small diamond crystallite. It has a mean C–C bond length of 1.52Å and an average bond angle of 109.14° (compared with 1.54 Å and 109.5° for diamond). The local electronic density of state (LDOS) of this cluster (Fig. 2B) shows a clear semiconducting gap of >5 eV (compared with 2.85 for the entire cell and 5.5 eV for diamond).

Thus, our calculations show that a diamond-like sp^3 cluster could spontaneously form in an a-C:H matrix with a density and H concentration experimentally shown to be optimal for diamond nucleation (step **a**). The formation of this cluster is sensitive to the density and hydrogen concentration. Similar calculations performed for hydrogen-free a-C (different densities up to 3 g/cm^3) and for a-C:H with lower densities (1.3 to 2.4 g/cm^3) did not yield the spontaneous nucleation of a diamond-like cluster. The hydrogen is concentrated in the more porous parts of the cell and decorates the surface of the sp^3 clusters, mainly forming sp^3 C–H bonds. The validity of our DFTB simulations is strongly supported by recent ab initio simulations not related to diamond nucleation (*23*), which showed the same trends in smaller a-C:H cell with a density of 2.9 g/cm^2 and a 19 at%H.

Our MD calculations and those of Bilek *et al.* (*23*) show that the sp^3 cluster density is larger than $10^{14}/cm^2$. The maximal observed nucleation density is 10^{10} nuclei/cm^2. The maximal formation probability of a perfect diamond cluster necessary for BEN is therefore 10^{-4}. This number cannot be substantiated by DF-based MD calculations but seems reasonable to achieve experimentally. We also expect that graphitic edges (*8*, *11*, *14*) (Fig. 1) and Si steps (*12*), form a "mold" for the perfect diamond clusters, increase the probability of their formation, and stabilize them.

In additional simulations, we found that the diamond-like sp^3 cluster can be annealed to a perfect diamond cluster. In the pathway shown in Fig. 3, interstitial carbon atoms are incorporated into the cluster, which is then terminated by either sp^3 C or H and forms a flawless diamond crystallite (*24*). The substantial diffusion of C interstitials and vacancies in diamond at 880°C (16) and the existence of C interstitials and H atoms in the evolving matrix (Fig. 2) strongly support such a mechanism and substantiate our suggested step **c**. (For further discussion of the substrate temperature effect, see SOM Note 6.)

In the final step **d**, the diamond cluster grows from ~30 atoms to $\sim 2 \times 10^4$ atoms. Banhart *et al.* (*25*) have shown that a graphitic layer covering a diamond crystal is transformed to diamond by MeV electron impact. They explained this transformation by preferential displacement (*15*, *16*). The displacement energy of sp^2 bonded atoms is considerably lower than that of sp^3 bonded atoms. The MeV electron bombardment (equivalent to H atoms with several hundred eV in the momentum transferred to carbon atoms), therefore, leaves the diamond atoms intact but displaces the graphitic atoms, which can then occupy diamond positions. On the basis of these

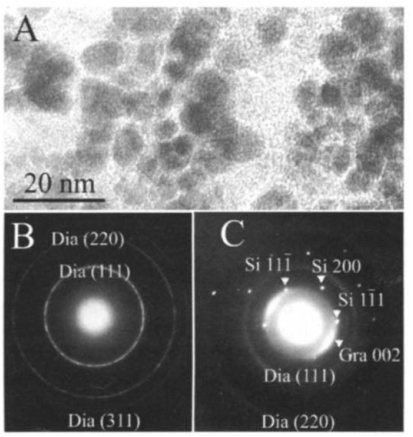

Fig. 1. (**A**) Cross-sectional HRTEM image of a film grown by prolonged hot filament bias-enhanced nucleation. (**B**) Planar view transmission electron diffraction (TED) pattern of the same film showing the diamond spacings. (**C**) Cross-sectional TED pattern of an ion beam–deposited film. In (A), ~5- to 10-nm diamond crystallites are embedded in the amorphous carbon matrix. Graphitic lobes in (C) are oriented graphitic planes associated with the diamond crystallites.

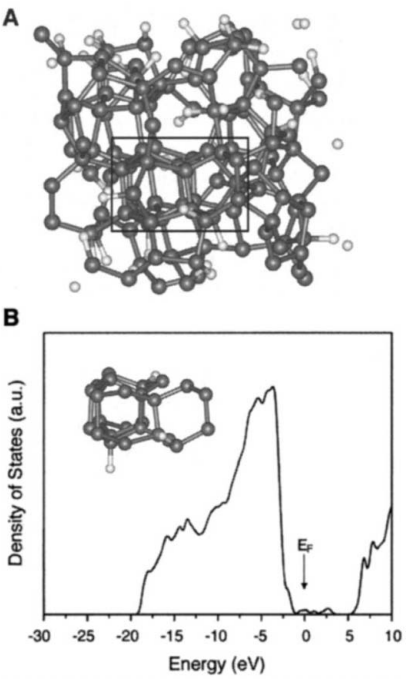

Fig. 2. (**A**) Structure of an a-C:H cell with 128 C atoms (gray) and 43 H atoms (white) (density 3 g/cm^2, 25 at%H) derived using tight-binding density functional calculations. A diamondlike cluster is observed in the center. The rest of the cell is less dense and the hydrogen tends to decorate the boundaries of the clusters. (**B**) The diamondlike cluster and its electronic density of states.

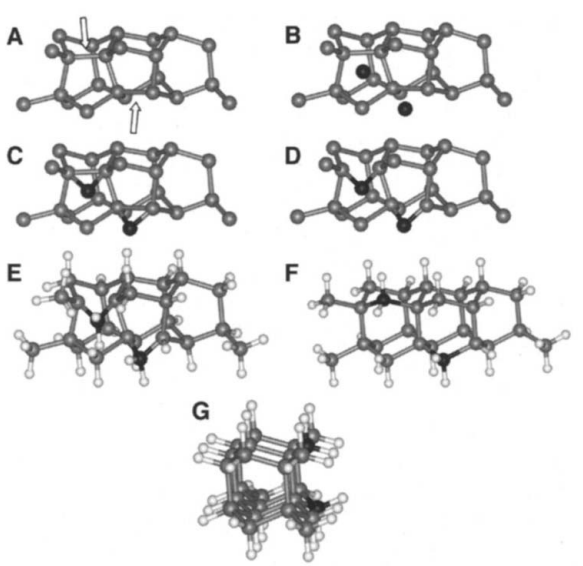

Fig. 3. A possible pathway from the diamondlike cluster to a perfect diamond cluster, derived from simulations. (**A**) The original cluster with the arrows indicating the reactive sites. (**B**) 2 C atoms (black balls) are added to the reactive sites. (**C**) The C atoms are bonded to their neighbors. (**D**) Previous bonds are broken and eliminated. (**E**) H termination is added (white balls) to all atoms with dangling bonds. (**F**) The structure relaxes to a perfect diamond cluster. (**G**) A rotated view of (F).

experimental findings, we suggest that the continuous bombardment of the evolving film during the BEN process induces the further growth of the diamond embryo by preferential displacement and transformation of amorphous carbon to diamond at the interface between the two phases.

Under typical BEN conditions, the H_2 content in the plasma is >90 to 99%, so that each deposited carbon atom is bombarded by 20 to 200 H atoms. The energy transferred by the colliding H atoms (<1/3 of the H energy) is below the displacement energy of diamond of ~35 to 40 eV (*25*) but larger than that of graphite [~25eV (*25*)]. Even if the displacement efficiency of one H atom is low [~10% per 200 eV (16)], each graphitic atom will be displaced several times by the total number of the bombarding H atoms and imparted a considerable probability of occupying a diamond position. Further support for this picture of diamond growth in the bulk by transformation of a-C atoms at the diamond–a-C interface comes from our TEM (Fig. 1) and near edge x-ray absorption fine structure (NEXAFS) (*8*, *11*) observations, which show that the diamond crystallites formed in BEN are always embedded in an a-C matrix and the diamond crystallite surface is never exposed in BEN. We could not find any evidence for diamond surface nucleation.

Once the diamond nucleus has reached a critical size, The BEN is stopped and the plasma is switched to nonbiased regular CVD conditions, in which the diamond crystallite grows via a CH_3/C_2H_2 radical surface growth mechanism (*1–3*), whereas the sp^2 bonded phases are etched by the harsh atomic hydrogen environment, exposing the buried perfect diamond crystallites for further growth. We have performed such a nonbiased CVD process for all the three sets of films reported here, and we have succeeded in growing polycrystalline diamond films.

The diamond crystallites that precipitate in the a-C:H matrix (sometimes on the graphitic edge, which serves as a nucleation site) are randomly oriented. Epitaxial growth is expected and observed for nucleation on Si steps, as established in our previous work (*12*). In this case, the epitaxy is a bulk process achieved through a "mold effect" (*12*, *15*, *16*), that is, the boundary conditions imposed by the crystalline structure of the Si step.

Previous attempts to understand diamond nucleation (*9*, *26–28*) considered either gas phase or surface nucleation. Under BEN conditions, clusters that form on the surfaces or nucleate in the gas phase and stick to the surface are not likely to survive the harsh energetic bombardment. In contrast, a diamond nucleus precipitated in the bulk is stabilized and protected from the bombardment of energetic species.

Although this report specifically addresses diamond nucleation in BEN, it can be extended to the nucleation of a host of metastable high-pressure phases of other materials. For example, all steps of our present model apply to the nucleation of cubic boron nitride (cBN) with energetic species, which is readily explained by the formation of cBN clusters in the matrix formed by subplantation (which includes edges of hexagonal BN planes). Similar to BEN of diamond, the cBN crystallites are always covered by a hexagonal BN layer and are never exposed on the surface (*29*), indicating their bulk precipitation nature.

References and Notes

1. J. C. Angus, C. C. Hayman, *Science* **241**, 643 (1988).
2. A. Paoletti, A. Tucciarone, Eds., *The Physics of Diamond*, Int. School of Physics, "Enrico Fermi" Course 135 (IOS Press, Amsterdam, 1997).
3. D. M. Gruen, I. Buckley-Golder Eds., *MRS Bull.* **23** (no. 9), 16 (1998).
4. F. P. Bundy, H. T. Hall, H. M. Strang, R. H. Wentroff, *Nature* **176**, 51 (1955).
5. J. Butler, H. Windischmann, *MRS Bull.* **23** (no. 9), 22 (1998).
6. S. Yugo, T. Kania, T. Kimura, T. Muto, *Appl. Phys. Lett.* **58**, 1036 (1991).
7. X. Jiang, C. P. Klages, R. Zachai, M. Hartweg, H. J. Fusser, *Appl. Phys. Lett.* **62**, 3438 (1993).
8. M. M. Garcia *et al.*, *Appl. Phys. Lett.* **72**, 2105 (1998).
9. M. M. Garcia, I. Jimenez, O. Sanchez, C. Gomez-Alexandre, L. Vazquez, *Phys. Rev. B.* **61**, 10383 (2000).
10. I. Gouzman, I. Lior, A. Hoffman, *Appl. Phys. Lett.* **72**, 296 (1998).
11. A. Hoffman, A. Heiman, S.H. Christiansen, *J. Appl. Phys.* **89**, 576 (2001).
12. S. T. Lee *et al.*, *Science*, **287**, 104 (2000).
13. W. J. Zhang *et al.*, *Phys. Rev. B* **61**, 5579 (2000).
14. W. R. Lambrecht *et al*, *Nature* **364**, 607 (1993).
15. Y. Lifshitz, S. R. Kasi, J. W. Rabalais, *Phys. Rev. Lett.* **62**, 1290, (1989).
16. _____, W. Eckstein, *Phys. Rev. B* **41**, 10468 (1990).
17. Y. Lifshitz, *Diam. Rel. Mater.* **8**,1659 (1999).
18. Optimal BEN conditions are found by performing a subsequent 1-hour CVD growth step in which large diamond crystallites are formed and their maximal nucleation density (crystallites per cm^2) can be determined.
19. G. Seifert, E. Eschrig, *Phys. Status Solidi* **127**, 573 (1985);
20. _____, W. Bieger, *Z. Phys. Chem.* **267**, 529 (1986),
21. D. Porezag, Th. Frauenheim, Th. Köhler, G. Seifert, R. Kaschner, *Phys. Rev. B* **51**, 12947 (1995).
22. J. Widany, F. Weich, Th. Köhler, D. Porezag, Th. Frauenheim, *Diam. Rel. Mater.* **5**, 1031 (1996).
23. M. M. M. Bilek, D. R. McKenzie, D. G. McCulloch, C. M. Goringe, *Phys. Rev. B* **62**, 3071 (2001). These ab initio simulations, performed to study a-C:H structure and not diamond nucleation, show the same trends as our calculations (a large coordination number, the formation of hydrogen-free sp^3 clusters, and H decoration of the cluster surface). These calculations independently verify our present data, but the small cell size (52 C atoms compared with 128 C atoms in our cell) does not allow observing large (27 C) diamondlike carbon clusters and inhibits the comparison of the C clusters to perfect diamond.
24. The reactivity of local structure was derived by Hartree-Fock calculations with a 3-21G basis set (*30*) and using a frontier orbital theory (*31*). The sites in the nanodiamond cluster where the HOMO (the highest occupied molecular orbital) is maximum have the highest reactivity for a carbon atom. The relaxation of the final hydrogen terminated structure was calculated by DFTB MD with the conjugated gradient approach.
25. F. Banhart, *Rep. Progr. Phys.* **62** 1181 (1999).
26. Y. Bar-Yam, T. D. Moustakas, *Nature* **342** 786 (1989).
27. P. Badziag, W. S. Verwoerd, W. P. Ellis, N. R. Greiner, *Nature* **343** 244 (1990).
28. N. M. Hwang, J. H. Hahn, D. Y. Yoon, *J. Cryst. Growth* **160** 87 (1996).
29. P. B. Mirkarimi, K. F. McCarty, D. L. Medlin, *Mater. Sci. Eng.* **R21**, 47 (1997).
30. J. S. Binkley, J. A. Pople, W. J. Hehre, *J. Am. Chem. Soc.* **102**, 939 (1980).
31. R. Hoffmann, *Rev. Mod. Phys.* **60**, 601 (1988).

32. Supported in part by the Research Grants Council of Hong Kong (grant 1051/00E), the Strategic Research Grants of City University of Hong Kong, and the Israeli Academy of Sciences.

Supporting Online Material

www.sciencemag.org/cgi/content/full/297/5586/1531/DC1
SOM notes 1 to 6
References

31 May 2002; accepted 15 July 2002

Oxidation-Resistant Gold-55 Clusters

H.-G. Boyen,[1]* G. Kästle,[1] F. Weigl,[1] B. Koslowski,[1] C. Dietrich,[1] P. Ziemann,[1] J. P. Spatz,[3] S. Riethmüller,[2] C. Hartmann,[2] M. Möller,[2] G. Schmid,[4] M. G. Garnier,[5] P. Oelhafen[5]

Gold nanoparticles ranging in diameter from 1 to 8 nanometers were prepared on top of silicon wafers in order to study the size dependence of their oxidation behavior when exposed to atomic oxygen. X-ray photoelectron spectroscopy showed a maximum oxidation resistance for "magic-number" clusters containing 55 gold atoms. This inertness is not related to electron confinement leading to a size-induced metal-to-insulator transition, but rather seems to be linked to the closed-shell structure of such magic clusters. The result additionally suggests that gold-55 clusters may act as especially effective oxidation catalysts, such as for oxidizing carbon monoxide.

Bulk gold is oxidation-resistant in air even at elevated temperatures. Nonetheless, gold can react with oxygen. For example, Au_2O_3 can be prepared electrochemically (*1*) or by exposure to highly reactive chemical environments such as ozone (*2*), atomic oxygen delivered by molecular dissociation at a hot filament (*3*), or radicals provided by an oxygen plasma (*4–6*).

Recently, it has been shown that the